Interfacial Adsorption and Aggregation Associated Changes in Secondary Structure of Human Calcitonin Monitored by ATR-FTIR Spectroscopy†

Horst H. Bauer,‡ Martin Müller,§ Jeannette Goette,§ Hans P. Merkle,‡ and Urs P. Fringeli*,§,∥

Department of Pharmacy, Swiss Federal Institute of Technology Zurich (ETH), Winterthurerstrasse 190, 8057 Zurich, Switzerland, Chemical Sensors, ETH-Technopark, Pfingstweidstrasse 30, 8005 Zurich, Switzerland, and Institute of Physical Chemistry, University of Vienna, Althanstrasse 14, P.O. Box 217, 1091 Vienna, Austria

Received February 24, 1994; Revised Manuscript Received June 21, 1994®

ABSTRACT: The peptide hormone human calcitonin (hCT) has a marked tendency to aggregate in aqueous solutions, resulting in viscous and turbid dispersions consisting of long fibrils approximately 80 Å in diameter. Both transmission (T-FTIR) and attenuated total reflection Fourier transform infrared (ATR-FTIR) experiments were applied on hCT adsorption and aggregation kinetics. By means of the surface sensitive ATR-FTIR spectroscopy at a hydrophobic/hydrophilic interface, early adsorption and aggregation steps of hCT could be followed in situ under real time conditions. Since the aggregation of hCT is associated with conformational changes, the secondary structure sensitive amide I′-band (D_2O) could be used as a diagnostic marker. ATR-FTIR spectra recorded during the aggregation kinetics of hCT showed an increase of the amide I′-band intensity by a factor of 3.4, interpreted as pronounced adsorption of hCT molecules from bulk solution to the germanium plate. Furthermore, variations in the line shape of the amide I′-band were interpreted. At the beginning, hCT adopted a random coil conformation followed by distinct formations of α-helical and intermolecular parallel β-sheet structures. Finally, the random coil content declined to 63%, whereas α and β contents rose to 8% and 29%, respectively. From our kinetics results the α-structures were formed faster than the β-structures. This was interpreted as an initial induction of amphiphilic helices during the adsorption process of hCT monomers. ATR-FTIR spectroscopy provides a sensitive analytical tool suggested to monitor interfacial adsorption and aggregation phenomena also of other peptides and proteins.

The formation and deposition of fibrous protein aggregates, or amyloid plaques, is characteristic of many diseases such as Alzheimer's disease, as reviewed by Lansbury (1992), and type II diabetes (Nishi et al., 1990). In the case of sickle cell disease, the polymerization of deoxygenated hemoglobin S to form aggregates leading to highly viscous gels is a well known primary event in its pathophysiology (Eaton & Hofrichter, 1987). Aggregation phenomena are also playing an important role in peptide and protein solution processing. Due to advances in biotechnology, the availability of highly active peptide and protein drugs is continuously increasing. In aqueous solutions many of these peptides and proteins tend to show marked physical instabilities, such as adsorption and aggregation phenomena upon processing, manufacturing of drug formulations, and during storage. Therefore, there is general interest in establishing sensitive analytical techniques to elucidate such adsorption and aggregation phenomena on a molecular level.

In this study, human calcitonin (hCT),[1] a 32 amino acid peptide hormone, was chosen as a model substance because hCT has a marked tendency to aggregate and precipitate in aqueous solutions. As a result viscous and turbid dispersions are obtained due to the formation of fibrils. Such fibrils are approximately 80 Å in diameter and up to several micrometers in length (Arvinte et al., 1993). Circular dichroism (CD) studies have shown that in water monomeric hCT has little ordered secondary structure at room temperature (Epand et al., 1983). However, studies of hCT fibrils using circular dichroism, fluorescence, and infrared spectroscopy revealed that fibrillated hCT molecules have α-helical and β-sheet secondary structure components (Arvinte et al., 1993). So far the quaternary structure of hCT fibrils is unknown.

Attenuated total reflection Fourier transform infrared spectroscopy (ATR-FTIR) represents a potentially useful interface-selective and highly sensitive method to monitor interfacial adsorption events in situ (Fringeli, 1992; Fringeli & Günthard, 1981). We expected adsorption at surfaces to be one of the causes leading to hCT aggregation. As described by Arvinte et al. (1993), aggregation and fibrillation of hCT is associated with significant changes in hCT secondary structure. Accordingly, the secondary structure sensitive amide I′ band in FTIR spectra may be used as a diagnostic marker for the initiation and progress of the hCT aggregation reaction. ATR-FTIR spectroscopy in combination with the conventional transmission (T)-FTIR technique should lead to more insight into conditions that influence hCT adsorption and aggregation phenomena. The ATR-FTIR technology may also provide a valuable tool to study adsorption and/or aggregation phenomena of other peptide and protein drugs.

MATERIALS AND METHODS

Materials. Synthetic human calcitonin (Figure 1) was supplied by Ciba Ltd., Basel, Switzerland. The freeze-dried powder contained hCT × 3 HCl with 1% (w/w) acetic acid.

† This work was supported in part by Ciba Ltd., Basel, Switzerland.
* Address correspondence to this author.
‡ Department of Pharmacy, Swiss Federal Institute of Technology Zürich (ETH).
§ Chemical Sensors, ETH-Technopark, Zürich.
∥ Institute of Physical Chemistry, University of Vienna.
® Abstract published in *Advance ACS Abstracts,* September 1, 1994.
[1] Abbreviations: CT, calcitonin; hCT, human calcitonin; IR, infrared; FTIR, Fourier transform infrared; ATR, attenuated total reflection; T, transmission; ν_0, center wavenumber; HWHH, half-width at half-height; CD, circular dichroism.

0006-2960/94/0433-12276$04.50/0 © 1994 American Chemical Society

1 5 10 15
Cys-Gly-Asn-Leu-Ser-Thr-Cys-Met-Leu-Gly-Thr-Tyr-Thr-Gln-Asp-

20 25 30
Phe-Asn-Lys-Phe-His-Thr-Phe-Pro-Gln-Thr-Ala-Ile-Gly-Val-Gly-Ala-Pro-NH_2

FIGURE 1: Sequence of hCT.

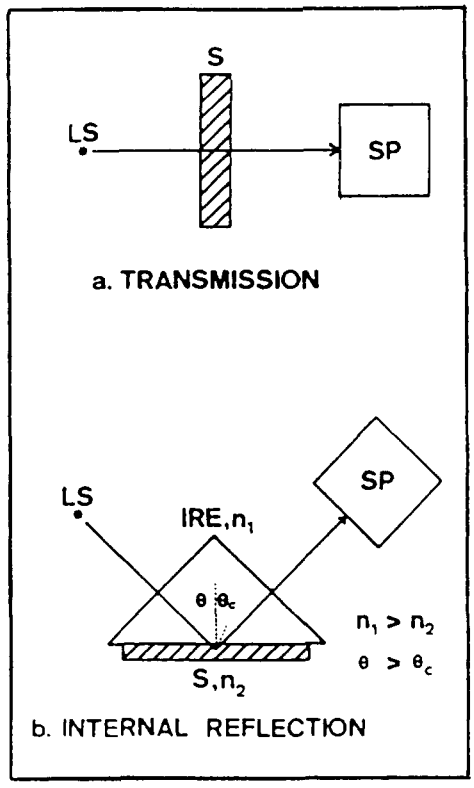

FIGURE 2: Comparison of transmission (a) with internal reflection (b) technique. LS, light source; S, sample; SP, spectrometer; IRE, internal reflection element (ATR crystal); θ, angle of incidence; θ_c, critical angle; n_1 and n_2, refractive indices of IRE and S, respectively [from Fringeli and Günthard (1981)].

Sample Preparation. In all experiments lyophilized hCT was dissolved in D_2O in a concentration of 10 mg/mL immediately before starting the individual experiments. No buffer salts were added to ensure rapid and complete dissolution of hCT. The pH value after dissolution of hCT was approximately 4.

Infrared Measurements. For comparison, both T-FTIR and ATR-FTIR experiments were performed (Figure 2). All measurements were made on a Bruker IFS 48 FTIR-spectrometer equipped with a MCT detector. Typically, spectra of 1024 scans were measured with a resolution of 4 cm^{-1}. The temperature in all experiments was kept at 25 °C.

For T-measurements the thermostated cuvettes with 25-μm BaF_2 windows were filled with freshly prepared hCT solution (10 mg/mL). Thereafter, aggregation was monitored with unpolarized IR light for 115 h. At the end of the experiment the cuvette was rinsed twice with D_2O, and a spectrum of the hCT material remaining adsorbed on the BaF_2 windows was recorded.

For the ATR-FTIR experiments a special ATR-IR accessory (Fringeli, 1989) was used. The measurements were performed on a polished and plasma-cleaned trapezoidal germanium plate (52 × 30 × 1 mm^3) with a refractive index $n_1 = 4$ resulting in 38 active reflections. The incident beam was polarized by means of a KRS polarizer, the angle of incidence was $\theta = 45°$ with respect to the surface of the plate. The freshly prepared hCT solution (10 mg/mL) was filled into the thermostated ATR sample cell after rinsing twice with D_2O. The first 0.5 mL of the sample solution was used for additional rinsing. The time point immediately after filling the sample cell with the hCT solution was defined as the starting point of the kinetics measurements. Parallel and vertical polarized single channel ATR-FTIR spectra were subsequently recorded over a period of 98 h. Absorbance spectra were computed with the sample intensity and the previously recorded reference intensity of D_2O.

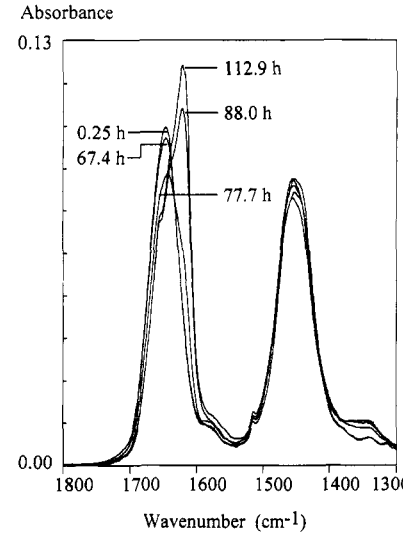

FIGURE 3: Time-dependent series of T-FTIR absorbance spectra recorded during the aggregation of dissolved hCT (10 mg/mL in D_2O). The time points at which the spectra were recorded are indicated.

Data Treatment. Both T- and ATR-FTIR absorbance spectra revealed different incompensation features in the secondary structure sensitive amide I′ and amide II′ region due to association vibration $\nu_A(D_2O)$ at about 1550 cm^{-1}. To overcome this problem reproducibly, scaled absorbance spectra of D_2O were subtracted from the original incompensated hCT spectra aiming at a horizontal baseline between 1800 and 1750 cm^{-1}.

Quantitative Analysis. As a quantitative separation technique of overlapped components in the structure sensitive amide I′-band, the curve fitting with Gaussian line shape according to the least-square condition was applied. The methodical procedure of the line shape analysis is summarized in the appendix (Müller, 1993).

RESULTS

Transmission FTIR Measurements. In a first approach to monitor the aggregation kinetics of hCT in solution, T-measurements were performed (Figure 2A). This technique weights surface and bulk solution phenomena rather equally. A selection of the kinetics set of baseline corrected T-FTIR spectra of a hCT solution in the amide range is presented in Figure 3. There the secondary structure sensitive dominant amide I′- and amide II′-bands appear between 1700 and 1600 cm^{-1} and between 1500 and 1400 cm^{-1}, respectively. Due to the D_2O solvent, the amide II band [60% δ(NH), 40% ν(CN)], which appears in the range 1560–1500 cm^{-1}, is shifted by about 100 cm^{-1} to cause the so-called amide II′-band reflecting a complete H–D exchange of all hCT peptide protons. Correspondingly, the amide I band [80% ν(CO), 10% δ(NH), 10% ν(CN)] is shifted by about 10 cm^{-1} upon the H–D exchange to cause the amide I′-band. Generally, there was no marked increase in amide I′ intensity during the

Table 1: Averaged Line Shape Parameters, i.e., Center Wavenumber and Half Width at Half Height (HWHH), on the Basis of Representative T-FTIR Spectra of the hCT Aggregation Kinetics and Assignment to Secondary Structures[a]

	1	2	3	4
center wavenumber (cm^{-1})	1650 ± 2	1635 ± 1	1618 ± 1	1590
HWHH (cm^{-1})	20 ± 2	8 ± 1	9 ± 1	29
assignment	random coil	α-helix	β-sheet	$\nu_{as}(COO^-)$

[a] The errors of the secondary structure components are given.

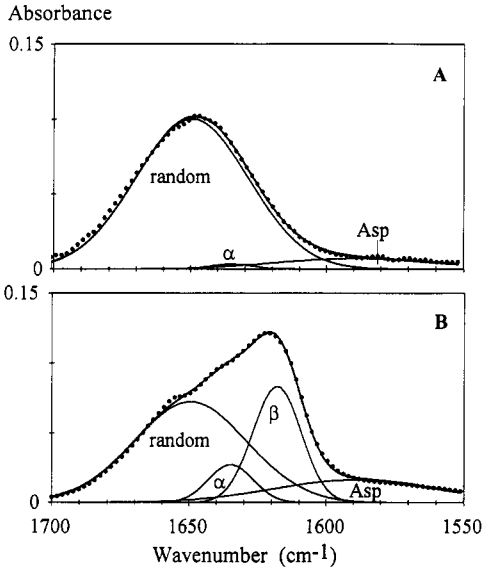

FIGURE 4: Curve fitting results of the amide I′-band of hCT in monomeric (A) and aggregated form (B) on the basis of four Gaussian components due to three secondary structures and the $\nu_{as}(COO^-)$ of Asp[15]. (A) Simulation of the first T spectrum recorded after 0.25 h, fitted predominantly with a broad Gaussian component at 1650 cm^{-1} due to random coil structure and a small α-helical component at 1635 cm^{-1}. (B) Simulation of the last measured T spectrum showing in addition to the random coil component significant components due to the ordered structures α-helix (1635 cm^{-1}) and β-sheet (1618 cm^{-1}).

experiment. The initial spectrum measured after 0.25 h of the aggregation series displayed a broad unstructured amide I′-band shape, which revealed no significant alterations up to approximately 67 h. Thereafter significant changes in the amide I′-band were observed (Figure 3).

In the case of hCT solutions, the quantification of the secondary structural contents was achieved by conventional curve fitting of the amide I′-bands (Ruegg et al., 1975) of all spectra recorded using a consistent parameter set (for parameter finding, see Appendix). The resulting parameter set is summarized in Table 1. By line shape analysis of the amide I′ region of the initially measured spectrum (Figure 4A) and of the last measured spectrum (Figure 4B), three amide I′ components at 1650, 1635, and 1618 cm^{-1} and one further component at 1590 cm^{-1} were found.

The initial spectrum of the series measured after 0.25 h could be simulated with one broad Gaussian component at 1650 cm^{-1} and a minor contribution of a component at 1635 cm^{-1}. Since the 1650-cm^{-1} component is broad (HWHH = 20 cm^{-1}) and CD measurements (Epand et al., 1983) reported predominantly random coil structure of hCT in freshly prepared aqueous solutions, we assigned this component to random structure. Considering an isotope shift of about 10 cm^{-1}, this is in good accordance to the expected frequency values of polypeptides in the random coil structure in H_2O around 1660 cm^{-1} (Miyazawa & Blout, 1960; Krimm, 1962)

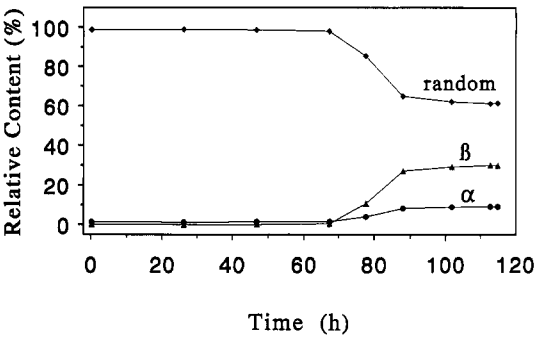

FIGURE 5: Variations of the secondary structures of hCT depending on the aggregation time, detected by the T-FTIR technique. Relative contents of the secondary structures (α, α-helix; β, β-sheet; random, random coil) computed as the quotient between the componental areas and the area of the total amide I′-band are plotted versus time.

and of about 1645 cm^{-1} (Susi & Byler, 1986) for a random protein structure in D_2O (see Discussion). The component at 1590 cm^{-1} was assigned to $\nu_{as}(COO^-)$ absorptions due to the carboxylic groups of acetate (see Materials and Methods) and of the only aspartate in the hCT amino acid sequence.

After 67 h a sharp increase of the component at 1635 cm^{-1} was observed, and a new component at 1618 cm^{-1} was formed, whereas the random coil component at 1650 cm^{-1} decreased. An unambiguous assignment of the component at 1618 cm^{-1} to β-sheet structure is possible. In H_2O the corresponding band is expected in the 1630-cm^{-1} region (Miyazawa & Blout, 1960; Susi & Byler, 1986; Krimm, 1962). Since our measurements have been performed in D_2O, a shift of about 10 cm^{-1} to lower values has to be taken into account (complete H–D exchange; see Figure 3).

Finally, we assign the 1635-cm^{-1} amide I′ component to an α-helical secondary structure. In H_2O the α-helix is expected to absorb in the range of 1650– to 1660 cm^{-1} (Miyazawa & Blout, 1960; Susi & Byler, 1986; Krimm, 1962). Taking the H–D isotope shift into account, our frequency is still rather low. However, it is well established by combined CD and IR measurements in D_2O, that homopolypeptides in the α-helical state can absorb in the range of 1641–1633 cm^{-1} (Chirgadze & Brazhnikow, 1974).

The time-dependent secondary structural alterations revealed a rather step-like behavior between 67 h and about 90 h (Figure 5). Among them, the relative content of the random coil structure declined within about 21.5 h from almost 100% to 60%, whereas the α-helical and β-sheet fractions rose both from appproximately 0% to 10% and to 30%, respectively. To check adsorption of the peptide onto the BaF_2 window material, an additional spectrum was recorded after rinsing the transmission cuvette twice with D_2O. It was subtracted from the last recorded spectrum of the aggregation series resulting in a difference spectrum with more or less poor signal intensities.This showed that practically complete adsorption of hCT from bulk solution to the BaF_2 windows had occurred.

ATR-FTIR Measurements. A sequence of the baseline corrected ATR-FTIR spectra is displayed in Figure 6. Right from the start of the experiment, the amide I′-band increased, asymptotically approaching a limit after about 65 h (Figures 6 and 8). A total increase in intensity of the amide I′-band of hCT by a factor of about 3.4 within the experimental period could be observed. The intensity increase of the amide I′-band was accompanied by significant changes in its line shape (Figure 6).

For the line shape analysis of the amide I′ region the parameter set already developed for the T-spectra was used (Table 1). However, for an accurate curve fitting of the ATR-

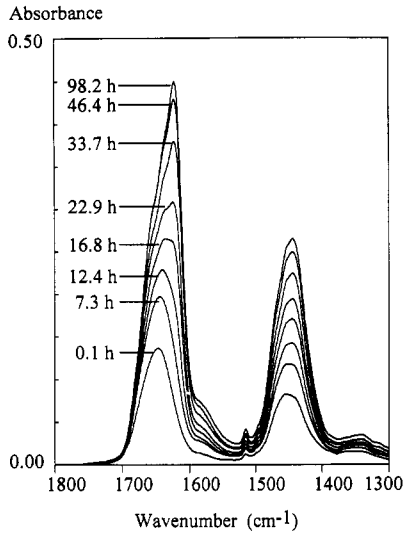

FIGURE 6: Series of ATR-FTIR absorbance spectra recorded during the aggregation of dissolved hCT (10 mg/mL in D_2O) at a germanium plate (38 active reflections, $\theta = 45°$, $n_1 = 4$). The time points at which the spectra were recorded are depicted.

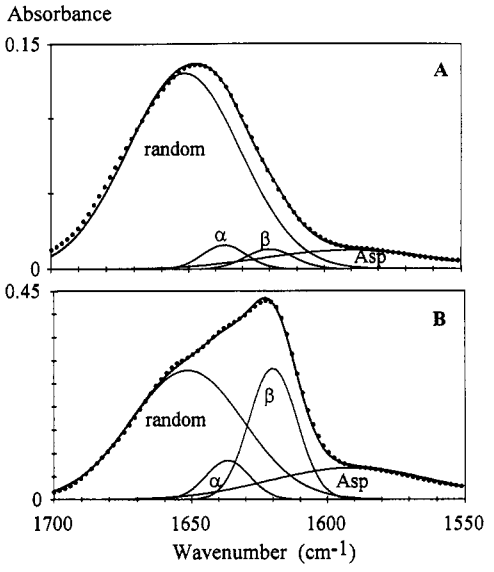

FIGURE 7: Curve fitting results of the amide I'-band of hCT in monomeric (A) and aggregated form (B) on the basis of four Gaussian components due to three secondary structures and the $\nu_{as}(COO^-)$ of Asp^{15}, detected by the ATR-FTIR technique. (A) Simulation of the first ATR spectrum recorded after 0.1 h, fitted predominantly with a broad Gaussian component at 1652 cm^{-1} due to random coil structure, with small amounts of ordered structures. (B) Simulation of the last measured ATR spectrum showing in addition to the random coil component significant components due to the ordered structures α-helix (1637 cm^{-1}) and β-sheet (1620 cm^{-1}).

FTIR spectra the center wavenumbers of the components of the T-spectra had to be shifted by +2 cm^{-1} (see Appendix). According to the T-spectra, the components at 1652, 1637, and 1620 cm^{-1} were assigned to the typical secondary structures, i.e., random coil, α-helix, and β-sheet, respectively. The fourth component at 1592 cm^{-1} was assigned to the $\nu_{as}(COO^-)$ absorptions mentioned above.

The initial ATR-FTIR spectrum measured after 0.1 h of the aggregation series could be simulated with one broad Gaussian component at 1652 cm^{-1} representing random coil structure, and small contributions of the α-helical component at 1637 cm^{-1}, of the β-sheet component at 1620 cm^{-1}, and of the $\nu_{as}(COO^-)$ component at 1592 cm^{-1} (Figure 7A). The

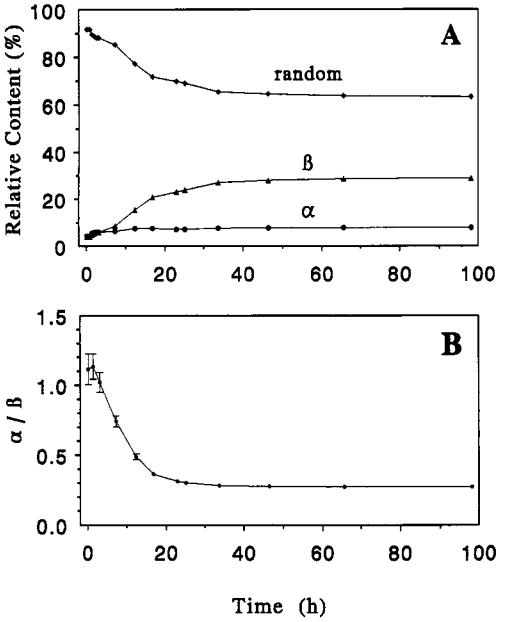

FIGURE 8: Variations of the secondary structures of hCT in dependence of the aggregation time, detected by the ATR technique. (A) Relative contents of the secondary structures (α, α-helix; β, β-sheet; random, random coil) computed as the quotient between the componental areas and the area of the total amide I'-band are plotted versus time. (B) Ratio between the α-helix and the β-sheet structure content versus time. The error bars indicate the statistical errors of the α/β ratio with 99% confidence limit based on the propagation of the errors of line shape analysis. Error bars are partly within symbols.

results of curve fitting of the last recorded ATR-FTIR spectrum of the time course is also presented (Figure 7B).

Significant time-dependent changes of secondary structures are presented in Figure 8. In contrast to the rather step-like feature observed in the T-experiments, the ATR-FTIR data exhibited continuous structural alterations from the very beginning. The intensity changes of the various secondary structure components are expressed as percentage of the total amide I' intensity in Figure 8A. During the time course of the experiment, the relative content of random coil structure declined rather continuously from approximately 92% to 63%. Simultaneously the α-helical and β-sheet fractions increased from 4% to 8% and from 4% to 29%, respectively.

To discriminate between the contributions of α-helical and β-sheet structures during the kinetics, the ratio between α-helix and β-sheet content is plotted versus time in Figure 8B. The error bars of the ratio values are related to the absolute errors of these two secondary structure contents, based on error propagation. Only at the beginning of the process did the rate of α-helix formation exceed that of β-sheet formation which, however, became dominant after about 2 h. Both structures approached a constant ratio after about 30 h.

Furthermore, the structural analysis revealed no formation of antiparallel pleated β-sheet structure, since there was no detectable signal between 1685 and 1675 cm^{-1} being a characteristic feature of β-antiparallel pleated sheet conformation (Miyazawa, 1960; Miyazawa & Blout, 1960; Krimm, 1962). Hence, only the formation of parallel pleated β-sheet structure can be concluded. The absence of antiparallel pleated β-sheet structure was also observed in the T-measurements.

DISCUSSION

In this study ATR-FTIR spectroscopy is introduced as a surface-sensitive technique to monitor induction and progress

of hCT adsorption and aggregation in situ. Recently, comprehensive studies focussing on conformational changes of hCT associated with the aggregation process in aqueous solution were presented (Arvinte et al., 1993). In nonfibrillating aqueous solutions hCT monomers provide a circular dichroism (CD) spectrum indicating an unordered secondary structure (Epand et al., 1983; Arvinte & Drake, 1993). However, according to previous CD investigations of Arvinte et al. (1993), hCT attains approximately 25% α-helical structure, if formation of fibrils takes place under so-called "large volume conditions", e.g., in a vial of 1 cm in diameter. These fibrils are referred to as "mature fibrils" by Arvinte and co-workers. Under restricted geometrical conditions (e.g., in a CD cuvette with a 10-μm path length) so-called "hindered fibrils" are formed revealing an α-helical content of only 17% (Arvinte et al., 1993). So far, quantifications on the β-sheet content of hCT molecules in fibrils are unavailable, because CD spectroscopy, in contrast to FTIR spectroscopy, is unable to precisely determine β-sheet contents. Because of the short path lengths used in these FTIR experiments, the α-helix content of hCT presented here has to be compared with that from CD investigations under restricted geometrical conditions, i.e., 17%.

It is well established that changes in the amide line shape correlate with secondary structure alterations of peptides or proteins (Miyazawa & Blout, 1960; Krimm, 1962; Krimm & Bandekar, 1986; Byler & Susi, 1986). According to these experimental studies and theoretical calculations, the IR amide modes of various secondary structures absorb at different frequencies. The typical secondary structures are mainly characterized by different hydrogen-bonding patterns whose energies are selectively detected by IR spectroscopy. Typically, the various amide components are strongly overlapped, hence they have to be separated and quantified by numerical techniques.

A well known advantage of IR spectroscopy is the reliable quantification of β-sheet conformation (Rüegg et al., 1975), whereas difficulties in separating the random coil from the α-helical contribution (Arrondo et al., 1993) have been reported. As a consequence equivocal assignments for random coil and α-helix are available in the literature (Miyazawa & Blout, 1961; Krimm, 1962; Krimm & Bandekar, 1986; Susi & Byler, 1986). This reflects two main problems of secondary structure determination by IR spectroscopy: The first results from poor separation of amide I,I′ components in the original spectrum due to band overlapping, which may lead to systematic errors by both methods, curve fitting (least-square analysis) and Fourier self deconvolution, respectively. The second problem results from the theoretical part. Since in the general case a molecule with N atoms results in $3N$–6 normal vibrations, it is very difficult, even with small peptides, to predict reliable information on the dependence of a normal vibration on the peptide structure. A further source for systematic errors results from the choice of the model band shape used for curve fitting (Gaussian, Lorentzian, mixtures: x Gaussian + $(1 - x)$ Lorentzian). In our analysis we have used pure Gaussian model line shapes, because only in this case our line shape analysis of the spectrum of freshly dissolved hCT resulted in a nearly complete random coil amount as reported by CD analysis (Epand et al., 1983). Since we consider the CD data to be more reliable in this case (dissolved molecules of random coil structure), we have used the CD information to adjust our model line shape (for more details, see Appendix).

In the case of hCT the evolving amide I′-band of aggregating hCT provided a set of well structured line shapes implying three partly resolved components, which could be significantly assigned to the three typical secondary structures, i.e., random coil, α-helix, and β-sheet, respectively (see above).

In a first approach the kinetics of hCT aggregation with T-FTIR measurements was studied. There were no marked changes in amide intensities during the experimental period. However, with a significant lag phase, after 67 h the T-FTIR results exhibited a sharp sigmoidal transition due to the formation of the different secondary structures, i.e., α-helix and β-sheet (Figure 5). Whereas the initial state can be attributed nearly completely to random coil structure representing hCT monomers in aqueous solution (Figure 4A), the formation of ordered secondary structures has to be interpreted as progressive aggregation of hCT. These results are in line with recent findings (Arvinte & Drake, 1993; Arvinte et al., 1993).

The demonstrated identity between the last spectrum of the kinetics series monitored by T-FTIR and that of the window-adsorbed hCT after rinsing the cuvette (see Results) gave evidence for total and, under the conditions used, irreversible adsorption of hCT material onto the BaF_2 surface. This fact may indicate that adsorption and aggregation phenomena of hCT are critically influenced by the properties of the solid/liquid interface. Hence, using ATR spectroscopy the adsorption at the ATR crystal can be monitored selectively and more sensitively as compared to T-measurements.

With ATR-FTIR spectroscopy a total increase in intensity of the amide I′-band of hCT by a factor of about 3.4 could be recorded within the experimental period (Figure 6). This is interpreted as the result of pronounced adsorption of the hCT molecules from the bulk solution onto the ATR plate. The first measured spectrum after 0.1 h of the ATR-FTIR series demonstrates almost complete random coil structure with small α-helical and β-sheet contributions (Figure 7A). Subsequently to adsorption, structural changes were induced featuring a continuous decrease in random coil structure accompanied by a marked increase in ordered secondary structures, i.e., α-helix and β-sheet. This formation of ordered structures of hCT correlates with the process of aggregation in agreement with recent circular dichroism and fluorescence studies on hCT aggregation and fibrillation phenomena. These studies have revealed that hCT molecules adopt α-helical and β-sheet structure components in fibrils (Arvinte et al., 1993).

The ATR-FTIR results (Figure 8B) show that initially (0–2 h) more or less equal formation of α-helical and β-sheet structures occurred which was followed (2 to $\sim$ 40 h) by significant β-sheet formation. We propose that the first stage might be attributed to initial surface adsorption of hCT molecules. The amphiphilic peptide hCT concentrated at the ATR plate surface which, in contact with D_2O, provided an amphiphilic interface. Since hCT can adopt an amphiphilic α-helix (Epand et al., 1983; Doi et al., 1989), it is expected that at the ATR plate/D_2O interface induces α-helical conformation in hCT (Kaiser & Kezdy, 1983). In the second stage the adsorption process is suggested to be superimposed by an aggregation phenomenon which resulted in the enhanced formation of fibrils indicated by higher β-sheet content. Meanwhile the α-helix content remained essentially unchanged.

With both techniques, i.e., T and ATR, the initial state of hCT conformation is found almost completely as random coil structure, also the two final states can be described as identical. Whereas the T results provide a significant lag phase (about

67 h) followed by a rather step-like transition (Figure 5), the ATR technique monitors the kinetics of hCT adsorption and aggregation at the surface as a slow continuous process from the very beginning (Figure 8A). Concerning the two different onset times of the hCT aggregation reaction in the T and in the ATR experiment shown here, it has to be considered that in general aggregation reactions are statistically controlled and, therefore, the time course may not be fully reproducible.

Furthermore, as there was no characteristic signal between 1675 and 1685 cm^{-1}, the formation of antiparallel β-pleated sheet structure had to be excluded. Hence, the β-sheet component formed during the hCT aggregation reaction is concluded to be a parallel β-pleated sheet structure. Because of the small size of the peptide, an intramolecular parallel β-sheet structure can be excluded, and, therefore, an intermolecular β-sheet arrangement of hCT molecules within the fibrils is proposed.

Finally, it should be noted that no carboxylic acid groups (COOH) could be detected at $\sim$1730 cm^{-1} although the pH of the sample solution was about 4. This may be explained by the formation of either intramolecular salt bridges within hCT monomers or intermolecular ones within hCT aggregates.

Future investigations should clarify whether the surface adsorption and aggregation tendency of hCT revealed in this study could be attenuated by modifying the properties of contact surfaces. Since the β-sheet formation is indicative of hCT aggregation, ATR-FTIR can be used to analyze the aggregation behavior of hCT at different surfaces. For insulin and other protein formulations it could be shown that hydrophilic container materials appear more compatible with protein physical stability than hydrophobic ones (Sefton & Antonacci, 1984; Nagaoka & Nakao, 1990). A specially formulated "pump" insulin preparation, when stabilized by addition of polyethylene–polypropylene glycol, was significantly more stable with respect to adsorption and aggregation (Feingold et al., 1984). As FTIR spectroscopy combined with the ATR technique offers both high sensitivity and surface selectivity, it may provide a powerful method to study surface adsorption and aggregation phenomena of peptides and proteins at defined interfaces.

Here an ATR-FTIR technique is introduced to monitor conformational changes of a peptide hormone due to adsorption and aggregation in situ and under real time conditions. The significance of this study is further stressed by the aspect that calcitonins from various species and calcitonin analogues can interact with lipids through the formation of an amphiphilic helix. This property is a feature of many membrane active peptide hormones and may be related to their biological activity (Sargent & Schwyzer, 1986; Epand et al., 1983; Kaiser & Kezdy, 1983; Taylor, 1989; Taylor & Kaiser, 1986).

To gain information on CT conformation in the presence of membrane-bound receptors, studies have been reported characterizing hCT in different membrane mimicking solvents (Doi et al., 1989; Motta et al., 1991). In analogy to the interaction studies of local anaesthetics with phospholipid model membranes using the ATR-FTIR technique (Fringeli, 1992; Schöpflin et al., 1987), membrane binding properties of hCT and other peptide and protein drugs may be monitored directly and in situ under more realistic microenvironmental conditions. Moreover, the application of linear polarized incident light can be used to investigate molecular ordering of peptides and/or lipids adsorbed to the ATR plate (Fringeli et al., 1986).

ACKNOWLEDGMENT

We sincerely thank Dr. T. Arvinte and Dr. B. Galli from Pharmaceuticals Research and Development, Ciba Ltd., Basel, Switzerland, and Dr. P. Schurtenberger, Institute for Polymers, Swiss Federal Institute of Technology, Zurich (ETH), for helpful and constructive discussions. Also the generous support of Ciba Ltd., Basel, Switzerland, is gratefully acknowledged.

APPENDIX: PROCEDURE OF LINE SHAPE ANALYSIS

1. Spectral Material. D_2O-compensated FTIR absorbance spectra (measured via T and ATR) of the kinetics experiments were used. Additionally, the sum of the first and the last spectrum was analyzed.

2. Type of Line Shape. It should be noted that the type of line shape may critically influence the result of the quantitative analysis of the secondary structure sensitive amide I′-band. Since the amide I′-band of freshly dissolved hCT measured by the T-technique could be perfectly simulated with a broad Gaussian component at about 1650 cm^{-1} and a small component at 1635 cm^{-1} combined with a component at 1579 cm^{-1}, due to the $\nu_{as}(COO^-)$, Gaussian line shape was assumed throughout. On the other hand, four Lorentzian components were necessary to obtain an approximately adequate fit. Since CD measurements (Epand et al., 1983) report predominantly random coil structure of hCT in freshly prepared aqueous solutions, our decision for Gaussian line shapes in the case of hCT is justified.

3. Procedure and Parameter Finding. For the parameter finding, curve fitting with relaxation of all three line shape parameters, i.e., center wavenumber (ν_0), half width at half height (HWHH), and area (A), was applied on the first and the last spectrum of the T-FTIR series and on the sum of both.

The result of the analysis of the first measured spectrum is given above (see 2). The analysis of the last measured spectrum of the time course revealed a total of four Gaussian components. In addition to a broad component at 1651 and 1609 cm^{-1}, narrow components were found at 1636 and 1619 cm^{-1}. Analysis on the sum of the first and the last measured spectrum reproduced the signals above within a range of 1 cm^{-1} (broad 1650-cm^{-1} component; narrow components at 1635 and 1618 cm^{-1}) with exclusion of the broad 1589-cm^{-1} component.

Comparing the line shape results of the three analyzed spectra only small deviations with respect to wavenumber ($\Delta\nu_0$) and to half width at half height (ΔHWHH) of the three structure sensitive components were found. From the small standard deviations of the center wavenumbers and HWHH of the components at 1650, 1635, and 1618 cm^{-1}, we decided that three secondary structural components offer a consistent parameter set for quantification.

4. Quantification. For a reproducible quantification of secondary structures the corresponding line shape parameters of the three analyzed spectra were averaged and applied on the whole spectra series. The obtained parameter set is given in Table 1. For the quantitative curve fitting procedure, the center wavenumbers and the half widths at half height of the components were fixed and only the component areas were relaxed. With the approximation of equal absorption coefficients for all amide components the procentual fractions of the areas relative to the total area of the amide I′-band were interpreted as secondary structural contents. The errors of

the percentage values of the secondary structures were less than ± 0.3%.

5. Consistency. Since the number of components obviously involved in the aggregation kinetics can be estimated even by visual inspection of the well featured amide I′ line shape, four components seem to be reasonable. However, the application of the four estimated components on a systematic spectra series has to reveal physicochemical consistency. Consistency exists if the components used simulate the line shapes of all spectra sufficiently well only by variation of the component areas and if the areas plotted versus time exhibit a reasonable functional relation.

6. Wavenumber Shifts between T and ATR Spectra. When the parameter set developed at the T spectra was applied on the ATR spectra, a shift of 2 cm^{-1} to higher wavenumbers of all components has to be achieved in order to get the same quality of fit as obtained with T spectra. This wavenumber shift between the T and the ATR spectra can be explained by the influence of the optical constants of sample and ATR crystal (Harrick, 1967).

REFERENCES

Arrondo, J. L. R., Muga, A., Castresana, J., & Goni, F. M. (1993) *Proc. Biophys. Mol. Biol. 59*, 23.

Arvinte, T., & Drake, A. F. (1993) *J. Biol. Chem. 268*, 6408.

Arvinte, T., Cudd, A., & Drake, A. F. (1993) *J. Biol. Chem. 268*, 6415.

Byler, M., & Susi, H. (1986) *Biopolymers 25*, 469.

Chirgadze, Y. N., & Brazhnikow, E. V. (1974) *Biopolymers 13*, 1701–1712.

Doi, M., Kobayashi, Y., Kyogoku, Y., Takimoto, M., & Goda, K. (1989) in *Proceedings of the 11th American Peptide Symposium,* pp 1965, La Jolla, CA.

Eaton, W. A., & Hofrichter, J. (1987) *Blood 70*, 1245.

Epand, R. M., Epand, R. F., Orlowski, R. C., Schlueter, R. J., Boni, L. T., & Hui, S. W. (1983) *Biochemistry 22*, 5074.

Feingold, V., Jenkins, A. B., & Kraegen, E. W. (1984) *Diabetologia 27*, 373.

Fringeli, U. P. (1989) in *From Biological Activity to Structure*, (Schlunegger, U. P., Ed.) pp 241, Springer-Verlag, Berlin.

Fringeli, U. P. (1992) in *Internal Reflection Spectroscopy: Theory and Applications* (Mirabella, F. M., Ed.) pp 255, Marcel Dekker, New York.

Fringeli, U. P., & Günthard, H. H. (1981) in *Membrane Spectroscopy* (Grell, E., Ed.) Vol. 31, pp 270, Springer, Berlin.

Fringeli, U. P., Leutert, P., Thurnhofer, H., Fringeli, M., & Burger, M. M. (1986) *Proc. Natl. Acad. Sci. U.S.A. 83*, 1315–1319.

Harrick, N. J. (1967) in *Internal Reflection Spectroscopy*, Harrick Scientific Corporation, New York.

Kaiser, E. T., & Kezdy, F. J. (1983) *Proc. Natl. Acad. Sci. U.S.A 80*, 1137.

Krimm, S. (1962) *J. Mol. Biol. 4*, 528–540.

Krimm, S., & Bandekar, J. (1986) *Adv. Protein Chem. 38*, 181.

Lansbury, P. T., Jr. (1992) *Biochemistry 31*, 6865.

Miyazawa, T. (1960) *J. Chem. Phys. 32*, 1647.

Miyazawa, T., & Blout, E. R. (1960) *J. Am. Chem. Soc. 83*, 712.

Motta, A., Temussi, P. A., Wünsch, E., & Bovermann, G. (1991) *Biochemistry 30*, 2364.

Müller, M. (1993) Ph.D. Thesis 10422, Swiss Federal Institute of Technology, Zürich, Switzerland.

Nagaoka, S., & Nakao, A. (1990) *Biomaterials 11*, 119.

Nishi, M., Sanke, T., Nagamatsu, S., Bell, G. I., & Steiner, D. F. (1990) *J. Biol. Chem. 265*, 4173.

Rüegg, M., Metzger, V., & Susi, H. (1975) *Biopolymers 14*, 1465.

Sargent, D. F., & Schwyzer, R (1986) *Proc. Natl. Acad. Sci. U.S.A. 83*, 5774.

Schöpflin, M., Fringeli, U. P., & Perlia, X. (1987) *J. Am. Chem. Soc. 109*, 2375.

Sefton, M. V., & Antonacci, G. M. (1984) *Diabetes 33*, 674.

Susi, H., & Byler, M. (1986) *Methods Enzymol. 130*, 290.

Taylor, J. W. (1989) in *Proceedings of the 11th American Peptide Symposium,* pp 592, La Jolla, CA.

Taylor, J. W., & Kaiser, E. T. (1986) *Pharmacol. Rev. 38*, 291.